7-1-2009

Intrauterine growth restriction increases fetal hepatic gluconeogenic capacity and reduces messenger ribonucleic acid translation initiation and nutrient sensing in fetal liver and skeletal muscle.

Stephanie R Thorn

Timothy Regnault
Western University, tim.regnault@uwo.ca

Laura D Brown

Paul J Rozance

Jane Keng

See next page for additional authors

Intrauterine Growth Restriction Increases Fetal Hepatic Gluconeogenic Capacity and Reduces Messenger Ribonucleic Acid Translation Initiation and Nutrient Sensing in Fetal Liver and Skeletal Muscle

Stephanie R. Thorn,* Timothy R. H. Regnault,* Laura D. Brown, Paul J. Rozance, Jane Keng, Michael Roper, Randall B. Wilkening, William W. Hay, Jr., and Jacob E. Friedman

Departments of Pediatrics (S.R.T., T.R.H.R., L.D.B., P.J.R., J.K., M.R., R.B.W., W.W.H., J.E.F.) and Biochemistry and Molecular Genetics (J.E.F.), University of Colorado Denver, Aurora, Colorado 80045

Expression of key metabolic genes and proteins involved in mRNA translation, energy sensing, and glucose metabolism in liver and skeletal muscle were investigated in a late-gestation fetal sheep model of placental insufficiency intrauterine growth restriction (PI-IUGR). PI-IUGR fetuses weighed 55% less; had reduced oxygen, glucose, isoleucine, insulin, and IGF-I levels; and had 40% reduction in net branched chain amino acid uptake. In PI-IUGR skeletal muscle, levels of insulin receptor were increased 80%, whereas phosphoinositide-3 kinase (p85) and protein kinase B (AKT2) were reduced by 40%. Expression of eukaryotic initiation factor-4e was reduced 45% in liver, suggesting a unique mechanism limiting translation initiation in PI-IUGR liver. There was either no change (AMP activated kinase, mammalian target of rapamycin) or a paradoxical decrease (protein phosphatase 2A, eukaryotic initiation factor-2α) in activation of major energy and cell stress sensors in PI-IUGR liver and skeletal muscle. A 13- to 20-fold increase in phosphoenolpyruvate carboxykinase and glucose 6 phosphatase mRNA expression in the PI-IUGR liver was-associated with a 3-fold increase in peroxisome proliferator-activated receptor-γ coactivator-1α mRNA and increased phosphorylation of cAMP response element binding protein. Thus PI-IUGR is-associated with reduced branched chain amino acid uptake and growth factors, yet up-regulation of proximal insulin signaling and a marked increase in the gluconeogenic pathway. Lack of activation of several energy and stress sensors in fetal liver and skeletal muscle, despite hypoxia and low energy status, suggests a novel strategy for survival in the PI-IUGR fetus but with potential maladaptive consequences for reduced nutrient sensing and insulin sensitivity in postnatal life. **(*Endocrinology* 150: 3021–3030, 2009)**

Intrauterine growth restriction (IUGR) is a significant cause of fetal and neonatal mortality and morbidity (1, 2). Considerable experimental animal and human epidemiological data indicate that IUGR fetuses and neonates are strongly predisposed to the development of obesity, diabetes, and cardiovascular disease in later life (3–5). It has been hypothesized that an inadequate supply of nutrients, hypoxia, or reduced concentrations of anabolic hormones might force the IUGR fetus to down-regulate growth of certain tissues as a mechanism for survival at the expense of altered metabolic regulation in adulthood (6). Indeed, the IUGR fetal liver is smaller relative to the brain, indicating asymmetric growth and selective down-regulation of organ growth (7). Moreover, increased rates of endogenous glucose production in the fetus have been found in animal models of

ISSN Print 0013-7227 ISSN Online 1945-7170
Printed in U.S.A.

doi: 10.1210/en.2008-1789 Received December 24, 2008. Accepted March 23, 2009.
First Published Online April 2, 2009
* S.R.T. and T.R.H.R. contributed equally to this work.

Abbreviations: AKT, Protein kinase B; AMPK, AMP-activated kinase; BCAA, branched-chain AA; C/EBP, CCAAT/enhancer binding protein; CREB, cAMP response element binding protein; CYTOC, cytochrome C oxidase; dGA, days gestation age; eIF, eukaryotic initiation factor; 4EPB1, eIF4e binding protein; ERR, estrogen receptor-related protein; G6P, glucose-6-phosphatase; GSK, glycogen synthase kinase; HNF, hepatocyte nuclear factor; IR, insulin receptor; IRS, insulin receptor substrate; mTOR, mammalian target of rapamycin; PEPCK, phosphoenolpyruvate carboxykinase; PGC, peroxisome proliferator-activated receptor-γ coactivator; PI-IUGR, placental insufficiency intrauterine growth restriction; PI3K, phosphoinositide-3 kinase; PP2A, protein phosphatase 2A; SIRT1, sirtuin 1; S6K, S6 kinase; TBS-T, Tris-buffered saline containing Tween 20; YY1, yin-yang transcription factor 1.

IUGR and preterm human infants (8–10). These altered developmental patterns, if persistent into postnatal life, may well play an important role in the evolution of insulin resistance, diabetes, and predisposition to metabolic disease later in life in IUGR offspring (4, 6, 11).

Insulin is a major regulator of hepatic metabolism, including protein synthesis, glycogen synthesis, gluconeogenesis, and amino acid metabolism, processes that are required for normal organ growth and development. The cellular signals downstream from the insulin receptor (IR) and insulin receptor substrate proteins (IRS)-1/2 that control growth and metabolism include activation of the phosphoinositide 3-kinase (PI3K) and protein kinase B (AKT) pathways and the classic p44/p42 MAPK (ERK1/2) signaling cascade (12). Both pathways play an important role in activating mammalian target of rapamycin (mTOR), a major energy sensor that controls both mRNA translation and provides negative feedback to the insulin signaling cascade through inhibition of IRS1/2 (13, 14). Downstream from mTOR, mRNA translation initiation is controlled by regulation of eukaryotic initiation factor (eIF)4e, eIF4e binding protein (4EPB1), and p70 ribosomal protein S6 kinase (S6K) (14, 15). These pathways are highly regulated and sensitive to changes in oxygen, nutrient status, and cell stress via input from several major energy and stress sensors including AMP-activated protein kinase (AMPK), eIF(2α), and protein phosphatase 2A (PP2A) (16–18).

Recently it was reported in our sheep model of placental insufficiency IUGR (PI-IUGR) that late gestation PI-IUGR fetal sheep have increased expression of gluconeogenic enzymes, including phosphoenolpyruvate carboxykinase (PEPCK) and glucose-6-phosphatase (G6P), along with increased rates of hepatic glucose production compared with control fetuses (9). PEPCK gene transcription is regulated by several key transcription factors, including cAMP response element binding protein (CREB), members of the CCAAT/enhancer binding protein (C/EBP) family (C/EBPα and C/EBPβ), and the transcriptional coactivator peroxisome proliferator-activated receptor-γ coactivator (PGC)-1α (19–21). Importantly, CREB activation can also control gluconeogenesis in the longer term by increasing PGC1α expression (22). Sirtuin 1 (SIRT1), a nicotinamide adenine dinucleotide oxidation-dependent deacetylase, is another nutrient sensitive factor regulating metabolic processes such as gluconeogenesis and muscle fatty acid oxidation (21, 23–25). In addition to insulin, which acutely suppresses PEPCK transcription and gluconeogenesis, AMPK activation can also inhibit PEPCK expression and hepatic glucose production (26, 27). Consequently, impaired nutrient sensing through reduced SIRT1 or AMPK activity could be involved in up-regulation of hepatic glucose production in the PI-IUGR fetus.

We hypothesized that changes in key regulatory proteins involved in insulin signaling, nutrient sensing, and mRNA translation initiation are responsible for reduced fetal growth and increased hepatic glucose production rates in the PI-IUGR fetus. To evaluate this, we measured the expression of key proteins and mRNA transcripts regulating these pathways in the liver and skeletal muscle of late gestation PI-IUGR fetal sheep. We also measured fetal branched-chain AA (BCAA) uptakes and concentrations, hormone levels, and fetal oxygen dynamics. Our results indicate that the PI-IUGR fetal liver and skeletal muscle have positive changes in the proximal insulin receptor signaling pathway for glucose metabolism, yet unique mechanisms limiting mRNA translation, in the absence of activation of key energy sensors. The PI-IUGR liver also has marked increases in expression of gluconeogenic genes and nuclear regulatory factors. These data indicate that lack of fetal nutrient sensing could be an important mechanism early in development linking IUGR to the inability to appropriately sense and respond to changes in nutrients and metabolites and lead to excess nutrient storage, insulin resistance, and uncontrolled glucose production in postnatal life (3, 6, 28).

Materials and Methods

PI-IUGR sheep model and physiological study

Pregnant Columbia-Rambouillet ewes carrying singleton fetuses were purchased from a commercial breeder (Nebeker Ranch, Santa Monica, CA) and managed and studied under compliance with the Institutional Animal Care and Use Committee, University of Colorado Denver, at the Perinatal Research Center (Aurora, CO), accredited by the National Institutes of Health, the U.S. Department of Agriculture, and the American Association for Accreditation of Laboratory Animal Care. PI-IUGR fetuses were created by exposing pregnant ewes to elevated ambient temperature (40 C for 12 h, 35 C for 12 h) from about 38 d gestation age (dGA, term = ~147 dGA) to 120 dGA. Control fetuses were used from pregnant ewes exposed to normal ambient temperatures daily (25 C) during gestation and pair fed to the food intake of the PI-IUGR ewes. One control animal was not included in the physiological studies due to catheter failure.

At approximately 127 dGA, ewes underwent surgery for placement of fetal and maternal catheters as previously described (9, 29). At approximately 134 dGA, under normal ambient conditions, fetal measurements were collected. Four sets of blood samples were drawn simultaneously from the umbilical vein and fetal artery at 20-min intervals after reaching steady state. Umbilical blood flows were determined by the steady-state ethanol diffusion method (29–31). Umbilical oxygen, glucose, and amino acid uptake rates were calculated using the Fick principle, and the umbilical glucose-oxygen quotient was calculated as the molar ratio of the umbilical lactate and O_2 uptake multiplied by 6 (32, 33).

At the end of the measurement period, ewes were euthanized, and the gravid uterus was removed and dissected into fetal and placental components. Fetuses were weighed and crown-rump length measured (34). Fetal liver and brain were weighed. The fetal ponderal index [fetal weight (grams)/ crown-rump length^3) (cubic centimeres)] and fetal brain/liver ratio [brain weight (grams) to liver weight (grams)] were calculated. A biopsy of fetal liver and biceps femoris skeletal muscle was removed immediately and snap frozen in liquid nitrogen for later use.

Analysis of blood samples

Blood samples were analyzed for hematocrit, pH, PO_2 and PCO_2, oxygen saturation, and oxygen contest using a blood gas analyzer (9, 35). Ethanol concentrations were determined using a quantitative enzymatic UV determination method (29–31). Insulin was assayed from a pooled sample of the four steady-state draws using an ovine insulin ELISA kit (Alpco, Windham, NH). Plasma IGF-I was measured from the same pooled sample by RIA after extraction (Diagnostics Systems Laboratories, Inc., Webster, TX) (36). BCAA concentrations were determined in each of the four steady-state samples with a Dionex HPLC amino acid analyzer (Dionex, Sunnyvale, CA) (30).

Protein preparation and western immunoblotting

For whole-cell extracts, liver or muscle tissue (200 mg) was lysed and homogenized in 2 ml of cell lysis buffer containing 20 mM Tris, 150 mM $MgCl_2$, 1% Triton, 2 mM EDTA, 20 mM β-glycerophosphate, and protease and phosphatase inhibitors [2.5 mM NaPP, 10 mM NaF, 1 mM phenylmethylsulfonyl fluoride, 2 μg/ml aprotinin, 2 μg/ml leupeptin, and 2 μg/ml pepstatin, and 1× phosphatase inhibitor cocktails 1 and 2 (Sigma, St. Louis, MO)]. Homogenates were incubated on ice and cleared by centrifugation. For nuclear enriched protein extracts, liver tissue (50 mg) was lysed and homogenized in 0.5 ml of lysis buffer containing 25 mM Tris, 10 mM KCl, 1.5 mM $MgCl_2$, 0.5 mM dithiothreitol, and protease and phosphatase inhibitors. The homogenates were incubated on ice for 10 min and centrifuged at 4000 × *g* for 10 min. The supernatant was removed and the nuclear pellet was sonicated in 0.25 ml of nuclear lysis buffer containing 50 mM Tris, 400 mM NaCl, 1.5 mM $MgCl_2$, 0.5 mM dithiothreitol, 0.2 mM EDTA, and protease and phosphatase inhibitors. Nuclear lysates were cleared by centrifugation.

Protein concentrations were determined using a bicinchoninic acid protein assay (Pierce, Rockford, IL). Protein samples (40–75 μg) were electrophoresed in 10% polyacrylamide gels and transferred to polyvinylidene fluoride or nitrocellulose membranes. Membranes were blocked in Tris-buffered saline containing 1% Tween 20 (TBS-T) and 5% milk for at least 1 h and then transferred to primary antibody solutions and incubated overnight. Membranes were washed three times in TBS-T, incubated with the appropriate horseradish peroxidase-conjugated secondary antibody for 1 h, washed five times with TBS-T, and detected using horseradish peroxidase-mediated chemiluminescence and autoradiography. Primary antibodies against IR-β, IRS-2, IRS-1, SIRT1, hepatocyte nuclear factor (HNF)-4α, C/EBPα, and C/EBPβ were purchased from Santa Cruz Biotech (Santa Cruz, CA); antibodies against regulatory subunit of PI3K (p85), AKT1, AKT2, and laminin A/C were purchased from Upstate (Billerica, MA); antibodies against phosphorylated AKT (S473), mTOR, phosphorylated mTOR (S2448), AMPK, phosphorylated AMPK (T172), eIF2α, phosphorylated eIF2α (S51), S6K, phosphorylated S6K (S421/T424), ERK1/2, phosphorylated ERK1/2 (T202/Y204), regulatory subunit of PP2A(R), catalytic subunit of PP2A(C), PGC1α, CREB, and phosphorylated CREB (S133) were purchased from Cell Signaling (Beverly, MA); antibody against glycogen synthase kinase (GSK)-3β was purchased from BD Biosciences (San Jose, CA); and an antibody against β-actin was purchased from Mediummune (Gaithersburg, MD). The majority of these antibodies have been used previously in sheep samples (9, 37–39); for those that had not been, we observed immunoreactive signal at the expected molecular weight, indicating specificity.

Protein expression was quantified using scanned images and densitometric analyses (Scion Image Software, Frederick, MD). Data for each protein sample were expressed relative to the mean of the control group. For phosphorylated proteins, a ratio of the phosphorylated and total protein data were calculated. To evaluate for equal protein loading, β-actin (whole cell extracts) or laminin A/C (nuclear extracts) protein expression was determined and expression was invariant. For liver whole-cell extract samples, five control and eight PI-IUGR samples were prepared and at least four were run on each gel. For liver nuclear enriched extracts, only three control and five PI-IUGR fetal liver samples were prepared due to limited availability of tissue samples, and all were run on each gel. For muscle whole-cell extract samples, seven control and nine PI-IUGR samples were prepared, and at least five were run on each gel, as indicated in figure legends. In some cases, two gels were run to accommodate the number of samples, and in these cases, expression on each blot is relative to an internal control sample that was run on each gel. Experiments were performed at least twice for each antibody. Representative results are shown.

RNA isolation and real-time PCR

RNA was isolated from powdered liver tissue (30–50 mg) using Qiazol and the RNeasy minikit with on-column deoxyribonuclease I treatment (QIAGEN, Valencia, CA). Quality and integrity of RNA was determined using the Experion RNA system (Bio-Rad, Hercules, CA). Reverse transcriptase reactions were prepared using 2 μg of RNA and Superscript III RT with random hexamers (Invitrogen, Carlsbad, CA). Real-time PCR primers and assays were optimized for PEPCK, PGC1α, SIRT1, yin-yang transcription factor 1 (YY1), estrogen receptor-related protein (ERR)α, cytochrome C oxidase (CYTOC), IR-A, IR-B, and 18S rRNA as shown in supplemental Table 1, published as supplemental data on The Endocrine Society's Journals Online web site at http://endo.endojournals.org. A previously validated assay for G6P was used (9). Real-time PCRs were performed using 20 ng of diluted cDNA (2 ng for 18S assay), 500 nM of each primer (200 nM for 18S), and SYBR Green PCR mix (AbGene Thermo Fisher Scientific, Rockford, IL) on the iCycler iQ5 real time PCR instrument (Bio-Rad). A relative standard curve of pooled liver cDNA was generated (six standards prepared as 4-fold serial dilutions) and used for quantification of unknown sample expression. Results were adjusted to 18S expression and expressed relative to the average of the control group for each gene.

Hepatic glycogen measurements

Hepatic glycogen concentration was determined as previously described (9). Results are expressed as milligrams glycogen per gram wet weight liver tissue.

Statistical analysis

Student's *t* test for unpaired samples after *F* test for equality of variance between treatments was used to analyze physiological, protein expression, and gene expression data between the control and PI-IUGR group. If *F* test was significant, data were analyzed using a Student's *t* test for unpaired samples with unequal variance. Statistical significance was declared at $P < 0.05$, and $P < 0.10$ is indicated as statistical tendencies.

Results

Fetal characteristics in PI-IUGR

Fetuses in both groups were of similar gestational ages at study (133 dGA control *vs.* 134 dGA PI-IUGR). The PI-IUGR fetuses weighed 55% less (Table 1) and had a 60% reduction in liver weight compared with control fetuses (42.8 ± 5.2 PI-IUGR *vs.* 112.3 ± 6.4 g control, $P < 0.001$). The ponderal index was similar between both groups, yet the brain to liver ratio was significantly increased in the PI-IUGR fetuses (Table 1). Fetal arterial blood oxygen content, saturation, and partial pressure were reduced in the PI-IUGR fetuses (Table 1). Umbilical blood flow was decreased by approximately 35% in PI-IUGR fetuses (Table 1). Umbilical (net fetal) oxygen uptake rate also was reduced by 25% in PI-IUGR fetuses (Table 1). The PI-IUGR fetuses were hypoglycemic and hypoinsulinemic and had reduced circulating IGF-I concentrations (Table 1). Lactate concentrations and the umbilical glucose-oxygen quotient were not significantly different between the two groups (Table 1).

PI-IUGR is associated with reduced branched chain amino acid uptake and arterial concentrations

The umbilical (net fetal) uptake rate of all three BCAA was significantly reduced in PI-IUGR compared with control fetuses (Table 1). Arterial concentrations of valine and leucine were not significantly different between the two groups, but isoleucine concentration was significantly reduced in the PI-IUGR group (Table 1).

TABLE 1. Fetal measurements and metabolic parameters in late-gestation control and PI-IUGR fetal sheep

Variable	Control	PI-IUGR	*P* value
Fetal growth parameters			
Placenta weight, g	392.4 ± 31.5	154.8 ± 19.1	
Fetal weight, g	3796.9 ± 117.8	1680.4 ± 178.2	<0.0001
Brain to liver ratio	0.42 ± 0.03	1.06 ± 0.12	<0.001
Ponderal index, g/cm^3	3.39 ± 0.25	2.83 ± 0.19	NS
Fetal arterial measurements			
Hematocrit	0.35 ± 0.01	0.37 ± 0.02	NS
pH	7.370 ± 0.004	7.330 ± 0.020	NS
O_2 content, mmol/liter	3.15 ± 0.19	1.38 ± 0.21	<0.001
O_2 saturation, %	49.23 ± 1.85	22.31 ± 3.02	<0.001
PO_2, mm Hg	18.96 ± 0.64	12.03 ± 0.76	<0.001
PCO_2, mm Hg	47.22 ± 0.57	51.38 ± 0.62	<0.001
Glucose, mM	1.14 ± 0.05	0.71 ± 0.05	<0.001
Glucose-oxygen quotient	0.56 ± 0.03	0.59 ± 0.02	NS
Lactate, mM	2.03 ± 0.09	4.71 ± 1.26	NS
Insulin, ng/ml	0.43 ± 0.10	0.19 ± 0.05	<0.05
IGF-I, ng/ml	54.5 ± 11.6	10.7 ± 3.2	<0.001
Valine, nmol/ml	462.0 ± 28.0	414.7 ± 30.5	NS
Leucine, nmol/ml	165.2 ± 6.5	174.0 ± 15.6	NS
Isoleucine, nmol/ml	106.5 ± 5.3	82.3 ± 7.8	<0.05
Umbilical blood flow and uptakes			
Blood flow, ml/min · kg	211.3 ± 11.9	145.3 ± 5.9	<0.001
Oxygen uptake, μmol/min · kg	0.35 ± 0.03	0.28 ± 0.01	<0.05
Valine uptake, μmol/min · kg	5.08 ± 0.98	2.66 ± 0.31	<0.05
Leucine uptake, μmol/min · kg	4.80 ± 0.52	3.05 ± 0.18	<0.05
Isoleucine uptake, μmol/min · kg	3.10 ± 0.34	1.67 ± 0.11	<0.01

Values are means ± SE for six control and 12 PI-IUGR fetuses. NS, Nonsignificant *P* value ($P > 0.05$).

PI-IUGR is associated with select changes in the proximal insulin signaling cascade

Protein expression changes in the fetal liver and skeletal muscle are summarized in Table 2. In the PI-IUGR fetal liver, expression of IR-β protein tended to be higher (Fig. 1A). Relative mRNA abundance for the IR-B transcript also tended to be increased by 50% (1.00 ± 0.09 control *vs.* 1.48 ± 0.21 PI-IUGR, $P = 0.06$), and there was no change in IR-A transcript abundance

TABLE 2. Summary of protein expression in liver and skeletal muscle in late-gestation control and PI-IUGR fetal sheep

	Liver			Skeletal muscle		
Protein	Control	PI-IUGR	*P* value	Control	PI-IUGR	*P* value
Proximal insulin signaling						
IR-β	1.00 ± 0.13	1.43 ± 0.16	0.07	1.00 ± 0.17	1.80 ± 0.30	<0.05
IRS-1/2	1.00 ± 0.10	0.78 ± 0.20	NS	1.00 ± 0.05	1.00 ± 0.20	NS
p85α	1.00 ± 0.04	0.86 ± 0.09	NS	1.00 ± 0.08	0.64 ± 0.11	<0.05
GSK3β	1.00 ± 0.21	0.38 ± 0.03	0.06	1.00 ± 0.02	0.77 ± 0.19	NS
AKT1	1.00 ± 0.39	0.86 ± 0.19	NS	1.00 ± 0.03	0.93 ± 0.03	NS
AKT2	1.00 ± 0.08	1.00 ± 0.10	NS	1.00 ± 0.13	0.63 ± 0.07	<0.05
Protein synthesis						
ERK1/2	1.00 ± 0.05	0.911 ± 0.05	NS	1.00 ± 0.04	1.02 ± 0.03	NS
P-ERK1/2	1.00 ± 0.27	1.201 ± 0.22	NS	1.00 ± 0.09	1.16 ± 0.19	NS
mTOR	1.00 ± 0.04	1.080 ± 0.08	NS	1.00 ± 0.35	1.55 ± 0.51	NS
P-mTOR	1.00 ± 0.14	1.130 ± 0.09	NS			
4EBP1	1.00 ± 0.20	2.500 ± 0.63	0.06	1.00 ± 0.28	0.99 ± 0.20	NS
eIF4E	1.00 ± 0.19	0.380 ± 0.07	<0.05	1.00 ± 0.33	1.31 ± 0.23	NS
S6K	1.00 ± 0.15	0.970 ± 0.15	NS	1.00 ± 0.08	0.99 ± 0.11	
Nutrient sensing and stress						
AMPK	1.00 ± 0.05	0.75 ± 0.11	NS	1.00 ± 0.04	0.91 ± 0.11	NS
P-AMPK	0.98 ± 0.27	2.04 ± 0.36	NS	1.00 ± 0.12	1.12 ± 0.10	NS
eIF2α	1.00 ± 0.13	1.12 ± 0.21	NS	1.00 ± 0.12	1.07 ± 0.12	NS
P-eIF2α	1.01 ± 0.12	0.54 ± 0.33	NS	1.00 ± 0.14	0.22 ± 0.03	<0.001
PP2AC	1.00 ± 0.09	0.47 ± 0.10	<0.005	1.00 ± 0.14	0.93 ± 0.07	NS
PP2AR	1.00 ± 0.04	0.94 ± 0.03	NS	1.00 ± 0.08	0.78 ± 0.07	<0.05

IRS-2 was measured in liver and IRS-1 was measured in skeletal muscle. Phosphorylation of proteins (P) is expressed as a ratio of phosphorylated to total levels as indicated in *Material and Methods*. Number of animals studied in each group is indicated in figure legends. Values are means ± SE. NS, Nonsignificant *P* value ($P > 0.05$).

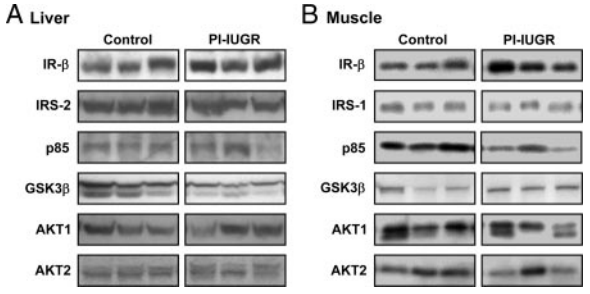

FIG. 1. Expression of components in the proximal insulin-signaling pathway in control and growth-restricted (PI-IUGR) fetal liver and skeletal muscle. The protein expression of IR-β, p85, IRS-2 (liver) or IRS-1 (muscle), GSK-3β, AKT1, and AKT2 was measured by Western blotting using whole-cell extracts prepared from late-gestation control and PI-IUGR fetal (A) liver and (B) skeletal muscle tissue samples. Western blot samples were quantified and analyzed for control (n = 4–5) and PI-IUGR (n = 4–6) fetal liver samples and for control (n = 5–7) and PI-IUGR (n = 6–8) fetal skeletal muscle as shown in Table 1. Representative images are shown for three control and three PI-IUGR samples.

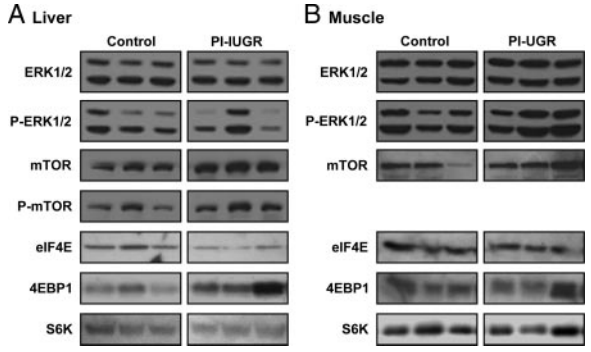

FIG. 2. Expression of proteins involved in protein synthesis in control and growth-restricted (PI-IUGR) fetal liver and skeletal muscle. The protein expression of ERK1/2, mTOR, 4EBP1, eIF4E, and S6K was measured by Western blotting using whole-cell extracts prepared from late-gestation control and PI-IUGR fetal (A) liver and (B) skeletal muscle tissue samples. Phosphorylation of ERK1/2 (P-ERK, T202/Y204), mTOR (P-mTOR, S2448), and S6K (P-S6K, S421/T424) was also measured. Western blot results were quantified and analyzed for control (n = 4–5) and PI-IUGR (n = 4–8) fetal liver samples and for control (n = 5–7) and PI-IUGR (n = 6–8) fetal skeletal muscle as shown in Table 1. Representative images are shown for three control and three PI-IUGR samples.

in the PI-IUGR compared with control fetal liver (1.00 ± 0.05 control *vs.* 1.21 ± 0.18 PI-IUGR). The expression of the proximal insulin signaling proteins, IRS-2 and p85α, was similar between the control and PI-IUGR liver (Fig. 1A). However, GSK3β, a negative regulator of insulin signaling, tended to be reduced by 60% in the PI-IUGR liver (Fig. 1A). The expression of the AKT1 and AKT2 proteins was similar between the control and PI-IUGR liver (Fig. 1A), and there was no change in basal AKT phosphorylation (serine 473, data not shown).

Compared with control fetuses, PI-IUGR fetal skeletal muscle had an 80% increase in the level of IR-β with no change in IRS-1 levels (Fig. 1B). Levels of p85α were reduced by 36% in PI-IUGR fetal skeletal muscle (Fig 1B). AKT2 levels were also reduced by 37% in the PI-IUGR compared with control fetal skeletal muscle, yet there were no significant differences in the levels of GSK3β or AKT1 (Fig 1B).

PI-IUGR alters expression and phosphorylation of proteins involved in mRNA translational initiation

We next evaluated the expression of proteins more distal in the insulin signaling pathway that are involved in the control of mRNA translation initiation. Phosphorylation of ERK1/2 protein and total levels of ERK1/2 protein were unchanged in the PI-IUGR compared with control fetal liver (Fig. 2A). The total levels of mTOR protein were also unchanged in the PI-IUGR fetal liver (Fig. 2A). The activity of mTOR, assessed by phosphorylation status, was similar between the control and PI-IUGR fetal liver (Fig 2A). Total levels of S6K were also unchanged (Fig. 2A). The protein expression of the translation initiation factor eIF4E was reduced by 60% in the PI-IUGR liver (Fig. 2A). The mean expression of 4EBP1, a binding protein and inhibitor of eIF4E, was increased by over 2-fold, although this failed to reach statistical significance (Fig. 2A). Thus, PI-IUGR fetuses may limit mRNA translation initiation in the liver by reducing levels of eIF4E and increasing levels of its inhibitor, 4EBP1.

In fetal skeletal muscle, there was no change in expression of ERK1/2 or mTOR or in phosphorylation of ERK1/2 (Fig. 2B). Phosphorylated mTOR protein was below the limits of detection by western blotting in fetal skeletal muscle. Moreover, levels of S6K, eIF4E, and 4EBP1 were unchanged (Fig. 2B), indicating that PI-IUGR had no effect on the levels of the effector proteins upstream or downstream of the mTOR pathway in fetal skeletal muscle.

Impaired nutrient and oxygen sensing signals in the PI-IUGR fetal liver and skeletal muscle

A major mechanism for sensing nutrient deprivation and hypoxia and thereby inhibiting protein translation initiation is the activation of AMPK. Both total and phosphorylated levels of AMPK protein were similar in the PI-IUGR compared with control fetal liver (Fig. 3A). Surprisingly, levels of phosphorylated eIF2α, a marker of endoplasmic reticulum stress, were paradoxically reduced in the PI-IUGR liver by 60%, whereas the total levels of eIF2α were unchanged (Fig. 3A). Also, the expression of stress kinase catalytic subunit PP2AC, a negative regulator of translation initiation, was reduced by 50%, with no change in expression of the regulatory subunit (PP2AR, Fig 3A).

In fetal skeletal muscle, there was no change in phosphorylation or expression of AMPK (Fig. 3B). Phosphorylated eIF2α protein was reduced by 75% in PI-IUGR skeletal muscle (Fig.

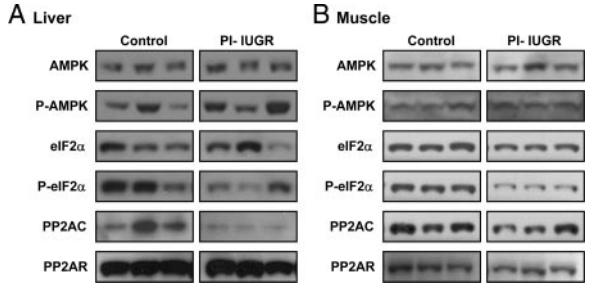

FIG. 3. Expression of nutrient and stress sensors in control and growth-restricted (PI-IUGR) fetal liver and skeletal muscle. The protein expression of AMPK, eIF2a, PP2AR, and PP2AC was measured by Western blotting using whole-cell extracts prepared from late-gestation control and PI-IUGR fetal liver (A) and muscle (B) tissue samples. Phosphorylation of AMPK (P-AMPK, T172) and eIF2α (P-eIF2α, S51) was also measured. Western blot results were quantified and analyzed for control (n = 4–5) and PI-IUGR (n = 4–8) fetal liver samples and for control (n = 5–7) and PI-IUGR (n = 6–8) fetal skeletal muscle as shown in Table 1. Representative images are shown for three control and three PI-IUGR samples.

3B). Levels of the regulatory subunit of the protein phosphatase, PP2AR, were decreased by 25%, yet levels of the catalytic subunit, PP2AC, were unchanged in PI-IUGR compared to control fetal skeletal muscle (Fig. 3B). These data indicate that major nutrient and oxygen-sensing mechanisms necessary for suppression of translation initiation were either not activated or changed in the opposite direction expected in the PI-IUGR fetal liver and skeletal muscle.

PI-IUGR induces gluconeogenic genes and related nuclear factors in fetal liver

PEPCK mRNA abundance was increased 20-fold and G6P expression increased 13-fold in the PI-IUGR fetal liver (Fig. 4A). The mRNA abundance of PGC1α was also increased 3-fold (Fig. 4A). The expression of CYTOC, a transcriptional target of PGC1α, was increased by nearly 2-fold (Fig 4A); however, there was no change in ERRα or YY1 expression, other downstream target targets of PGC1α (40). The mRNA abundance for the PGC1α activator SIRT1 was unchanged in the PI-IUGR fetal liver (Fig 4A). Furthermore, hepatic glycogen content was similar between the PI-IUGR and control fetuses (45.9 $\pm$ 6.8 mg/g PI-IUGR *vs.* 37.6 $\pm$ 4.8 mg/g control), suggesting fetal gluconeogenesis rather than glycogenolysis.

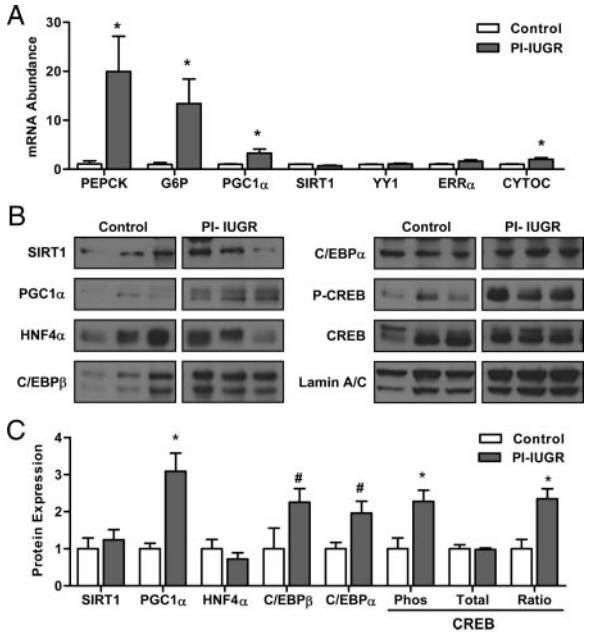

FIG. 4. Relative mRNA abundance and nuclear protein expression of gluconeogenic and regulatory genes in control and growth-restricted (PI-IUGR) fetal liver. A, The mRNA abundance for PEPCK, G6P, PGC1α, SIRT1, YY1, ERRα, and CYTOC was determined by real-time PCR. Results were adjusted for 18S rRNA abundance and expressed relative to the average of the control group (n = 5 control, n = 9 PI-IUGR fetal liver samples). Means $\pm$ SEM are shown for each group. B, The protein expression of SIRT1, PGC1α, HNF4α, C/EBPβ, C/EBPα, CREB, and phosphorylated CREB (P-CREB, S133) was measured by Western blotting using nuclear extracts prepared from late-gestation control and PI-IUGR fetal liver tissue samples. The expression of lamin A/C is shown as loading control. C, Western blot results were quantified and analyzed for control (n = 3) and PI-IUGR (n = 5) fetal liver samples. For CREB, phosphorylation was measured and quantification results are shown for the phosphorylated (Phos) and total form of the protein and a ratio of the phosphorylated to total protein levels. Means $\pm$ SEM are shown for each group. *, $P < 0.05$; #, $P < 0.10$.

Next, we evaluated the expression of these and other key gluconeogenic regulatory factors at the protein level in liver whole-cell and nuclear extracts prepared from control and PI-IUGR fetal livers. PGC1α expression was 3-fold higher in nuclear extracts from the PI-IUGR fetal liver, and phosphorylation of CREB was more than 2-fold higher in both whole-cell and nuclear extracts from the PI-IUGR liver, whereas total levels of CREB were similar (Fig. 4, B and C, and supplemental Fig. 1). Expression of C/EBPα and C/EBPβ also tended to be higher in nuclear extracts, whereas expression was similar in whole-cell extracts prepared from the PI-IUGR fetal liver (Fig. 4, B and C, and supplemental Fig. 1). The expression of SIRT1 and HNF4α was similar between the control and PI-IUGR fetal liver (Fig. 4, B and C, and supplemental Fig. 1). These data suggest that the fetal sheep PI-IUGR liver has a robust increase in PGC1α and factors that act through cAMP regulatory pathways controlling gluconeogenesis.

Discussion

Chronic fetal nutrient deprivation during late gestation, whether induced by placental insufficiency or maternal nutrient restriction, results in fetal growth restriction, decreased liver and skeletal muscle growth, and changes in hepatic function, including persistently increased gluconeogenesis, that increase the postnatal risk for development of diabetes and obesity (3, 4, 6, 41). The cellular mechanism(s) responsible in the IUGR fetus remain inadequately understood. Our results indicate that PI-IUGR is associated with decreased net fetal uptake rates of BCAA, hypoxia, reduced IGF-I, insulin, and glucose concentrations and a specific reduction in skeletal muscle AKT2 protein. We also found that the PI-IUGR fetus has a unique mechanism that may limit mRNA translation downstream of mTOR in the liver. The PI-IUGR fetal liver and skeletal muscle also show significant changes in the proximal insulin signaling pathway and unexpectedly no change or, in some cases, a paradoxical decrease in expression of nutrient and energy sensors. Furthermore, we found increased expression of key nuclear regulatory factors in the liver that may be responsible for increased glucose production in the PI-IUGR fetus. These changes may be necessary to allow the PI-IUGR fetus to survive but may also ultimately increase the risk for diabetes.

IUGR is associated with reduced fetal BCAA uptake

The concentration of isoleucine was significantly lower in the PI-IUGR fetal circulation, but the concentrations of leucine and valine remained normal despite reduced net fetal uptake rates of all three BCAAs. These data contrast with previous reports in this model showing no change in the concentrations or net fetal uptake rates of the BCAA (42). These differences likely represent variation in the PI-IUGR fetus due to different degrees of placental insufficiency. Maintenance of normal fetal arterial BCAA concentrations likely represents a balance among increased BCAA release from protein breakdown (42, 43), increased BCAA oxidation (42), and reduced amino acid use for protein synthesis (42). Because the BCAAs are rate limiting for protein synthesis, this implies that reduced BCAA availability along with

reduced blood oxygen content and reduced plasma insulin and IGF-I concentrations may suppress protein synthesis, leading to reduced skeletal muscle mass and fetal growth.

Decreased protein translation initiation

mTOR regulates cell growth by sensing upstream nutrient and hormonal signals to coordinate gene activation, protein synthesis, and cell growth (13, 14). mTOR phosphorylates 4EBP1 and S6K, which increases mRNA translation (13, 14). Interestingly, we found that despite nutrient and oxygen deprivation, mTOR phosphorylation was unchanged in the PI-IUGR fetal liver and undetectable in the PI-IUGR skeletal muscle. Likewise, the immediate upstream inputs that control mTOR activity, such as AMPK and AKT, were unchanged. The initiation phase of mRNA translation is a pivotal site of regulation for global rates of protein synthesis as well as a site through which the synthesis of specific proteins is controlled. The abundance of eIF4e, which is rate limiting relative to other components in the eIF4 complex, was reduced in the PI-IUGR liver and could be an important mechanism limiting translation initiation (44). Thus, our observations of increased 4EBP1 combined with reduced eIF4e could serve to limit mRNA translation initiation and growth in the PI-IUGR fetal liver. We did not find any changes in these proteins in the PI-IUGR fetal skeletal muscle suggesting that tissue-specific mechanisms are involved.

Our findings are consistent with data in another model of fetal growth restriction, showing that skeletal muscle from midgestation nutrient-restricted fetal sheep had no change in total levels of mTOR or AMPK protein, yet contrast with the finding of reduced phosphorylation of mTOR and a downstream target ribosomal protein S6 (45). We did attempt to measure the phosphorylation of several proteins, including mTOR, AKT, and S6K, but due to low basal activity levels in our fetal tissues, these results are not measurable. Studies are underway to evaluate the effect of insulin stimulation of these pathways.

Increased expression of the proximal insulin signaling pathway

The level of IR-β protein was increased in PI-IUGR skeletal muscle and tended to be increased at both the mRNA and protein level in the liver. Up-regulation of IR-β is perhaps not surprising, given the low levels of insulin in the PI-IUGR fetus. There was a decrease in the p85α regulatory subunit of PI3K in PI-IUGR fetal skeletal muscle. Decreased p85α is consistent with a potential for increased glucose uptake. Decreasing any of the regulatory subunits by genetic deletion in mouse models or by small interfering RNA in cell models leads to enhanced PI3K activity and downstream signaling (46), whereas an increase in the expression of p85α reduces insulin-stimulated PI3K activity and is associated with insulin resistance (47–49). A decrease in the p85α and p110 subunits has been reported in adult skeletal muscle from a protein-restricted IUGR rat model and in adults with low birth weight (50). Overall, the changes in IR-β and p85α are consistent with increased peripheral insulin sensitivity to glucose utilization observed previously in the PI-IUGR fetus *in utero* during a hyperglycemic clamp (9).

The decrease in AKT2 in the PI-IUGR fetal skeletal muscle is consistent with studies showing a distinct role of AKT2 on skeletal muscle differentiation and myogenesis (51–53). AKT1 is required for proliferation, whereas AKT2 promotes cell cycle exit (54). During differentiation *in vitro* and during regeneration *in vivo*, AKT2 expression and activity are markedly induced, suggesting a possible role of AKT2 during muscle proliferation (52, 55, 56). Indeed, in human skeletal muscle, IRS-1 and AKT2 are required for myoblast differentiation and glucose metabolism, whereas IRS-2 and AKT1 was used for lipid metabolism (57). Similarly, in AKT2 knockout mice, there is mild growth deficiency but also age-dependent loss of adipose tissue and severe diabetes, with neither AKT1 nor AKT3 knockout mice showing similar defects (58). These studies suggest that AKT2 down-regulation in fetal skeletal muscle in the PI-IUGR model could be an important factor limiting skeletal muscle growth *in utero*. This decrease may also be tissue specific because levels of AKT1 and AKT2 were not affected in the liver of the PI-IUGR fetus and unrelated to changes in skeletal muscle glucose metabolism because normal glucose-stimulated glucose utilization rates in the PI-IUGR fetus have been reported (9).

Impaired nutrient sensing in PI-IUGR fetus

One of the novel findings of the present study is that the late-gestation PI-IUGR fetus demonstrates a failure to activate major energy and stress sensors, including AMPK, mTOR, and SIRT1, and decrease in the levels of the stress kinase PP2A and eIF2α. These results may seem paradoxical, given that the fetus is exposed to hypoxia, and reduced glucose and anabolic hormones, but likely represent a unique adaptive mechanism. In the short-term, the regulation of protein phosphorylation by kinases and phosphatases is an important mechanism in the control of the apoptotic cell death program. For example, cells lacking nutrients suppress mTOR activity via AMPK activation and can also activate the autophagy machinery via SIRT1 activation and mTOR inhibition. These mechanisms provide cells with a source of energy, thereby enhancing cell survival during the stress (13, 17, 59, 60). In the long-term, however, chronic nutrient stress in cell culture systems through the activation of AMPK, PP2A, or eIF2α has been demonstrated to result in apoptosis and cell death (61, 62). Collectively, this suggests that the adaptations that we have shown in the PI-IUGR fetus may be important mechanism for survival outcome.

The decreased ability of the PI-IUGR fetus to activate cell nutrient and stress sensing pathways, however, could have important negative implications for the development of diabetes later in life if this change persists postnatally. For example, AMPK activation is linked to fatty acid oxidation through phosphorylation of acetyl CoA carboxylase (17, 63). AMPK activation also can reduce gluconeogenesis and PEPCK transcription via phosphorylation and nuclear removal of transducer of regulated CREB-2 and phosphorylation of GSK3β (26, 27). The inability of AMPK to suppress mTOR activity has been shown to lead to endoplasmic reticulum stress, apoptosis, and impaired insulin action (16). These data, together with our observations of normal hepatic glycogen levels in the PI-IUGR fetus despite low glucose supply and circulating glucose and insulin concentra-

tions (9), suggest that there may be a selective adaptation in the nutrient sensing pathways that if persistent postnatally would result in greater capacity for nutrient storage and presumably insulin resistance.

Induction of the gluconeogenic pathway in PI-IUGR liver

Consistent with increased glucose production in the PI-IUGR fetus (9), PEPCK mRNA abundance was increased 20-fold and G6P mRNA abundance increased 13-fold (Fig. 4). Glucose is the major energy substrate for fetal oxidative metabolism (64, 65). PI-IUGR results in hypoglycemia in the fetus, in part due to reduced placental glucose transport, up-regulation of glucose transporters (GLUT1 and GLUT4) and the proximal insulin pathway in several tissues (66) (results herein), and the development of asymmetric growth, which combine to increase glucose uptake and utilization capacity (9, 67, 68). The PI-IUGR fetus also prematurely up-regulates glucose production during late gestation (9). This is not enough, however, to meet the increased demand for glucose utilization in the fetus and the fetus remains hypoglycemic (9).

The molecular basis for chronic increased glucose production, despite normal to increased expression of proteins in the proximal insulin signaling cascade, may be due to induction of nuclear factors that increase gluconeogenic gene expression. PGC1α, a major coactivator that encodes a transcriptional pathway for increased gluconeogenesis (21), was increased by 3-fold in the PI-IUGR fetal liver. We also found a significant increase in the mRNA abundance for CYTOC, a transcriptional target of PGC1α (40). This suggests that PGC1α activity is increased in the PI-IUGR liver, consistent with its effects on PEPCK and G6P gene expression. We also found increased expression of phosphorylated CREB, which binds directly to the PEPCK promoter via the cAMP response element site and can activate PGC1α expression (22). The expression of C/EBPα and C/EBPβ, which also bind to the cAMP response element, tended to be increased in nuclear extracts prepared from the PI-IUGR fetal liver. This suggests that cAMP-dependent regulatory pathways may drive early gluconeogenic gene expression patterns in the PI-IUGR fetal liver. Indeed, the PI-IUGR fetus has been reported to have increased circulating concentrations of glucagon and norepinephrine that activate cAMP-dependent signaling pathways (7). These results are similar to those in another fetal sheep model of short-term (10 d) hypoglycemia, whereby the levels of PEPCK, phosphorylated CREB, and glucose production are increased during late gestation (37). These various observations implicate glucose deprivation as an important causative factor for IUGR-induced gluconeogenesis through a mechanism involving cAMP-driven signals, such as PGC1α, CREB, and C/EBP. Whether these are permanently modified as master regulatory factors in the postnatal period is the subject of ongoing investigation.

Summary and implications

Several studies have shown that IUGR fetal sheep have maintained or increased whole-body insulin sensitivity (9, 68, 69). In early postnatal life, ovine IUGR offspring undergo rapid growth, increased feeding activity, and development of adiposity in addition to maintained insulin sensitivity (70–72). As these ovine IUGR offspring mature, however, they have increased body weight gain and adiposity and develop glucose intolerance (70, 73). Moreover, IUGR fetal sheep and postnatal IUGR rodents have increased PEPCK and hepatic glucose production (9, 74, 75). These early increases in PEPCK and glucose production, however, contrast with increased peripheral insulin sensitivity in fetal and early postnatal life and suggest that chronically increased glucose production resulting from IUGR may contribute to the development of insulin resistance in postnatal animals. Future studies are underway to investigate the effect of insulin on these pathways to better understand the impact of nutrient and growth restriction *in utero*.

Overall, our data indicate that the PI-IUGR fetus has adapted to nutrient deprivation from reduced placental nutrient transport in unique ways to ensure survival. PI-IUGR is associated with reduced circulating hormones, decreased BCAA uptake rates, hypoxia, and reduced AKT2 levels, all of which contribute to reduced skeletal muscle mass and fetal growth. We also found up-regulation of the proximal insulin signaling pathway as a mechanism for increased glucose uptake. There is also up-regulation of nuclear regulatory factors promoting glucose production in the liver and failure to activate nutrient sensing pathways in both liver and skeletal muscle. These adaptations in IUGR offspring, however, may set the stage for cellular changes that underlie the progression to insulin resistance, uncontrolled glucose production, diabetes, and increased nutrient storage in postnatal life.

Acknowledgments

We are thankful to David Caprio and Karen Trembler at the Perinatal Research Center for technical assistance.

Address all correspondence and requests for reprints to: Jacob E. Friedman, Departments of Pediatrics and Biochemistry and Molecular Genetics, University of Colorado Denver, Mail Stop F-8106, P.O. Box 6511, Aurora, Colorado 80045. E-mail: jed.friedman@ucdenver.edu.

This work was supported by National Institutes of Health Grants HD41505-02 (to T.R.H.R. and R.B.W.), DK52138 (to W.W.H.), DKF32-082207 (to S.R.T.), and K068590 (to J.E.F.).

Disclosure Summary: The authors have nothing to declare.

References

1. **Brar HS, Rutherford SE** 1988 Classification of intrauterine growth retardation. Semin Perinatol 12:2–10
2. **Pollack RN, Divon MY** 1992 Intrauterine growth retardation: definition, classification, and etiology. Clin Obstet Gynecol 35:99–107
3. **McMillen IC, Robinson JS** 2005 Developmental origins of the metabolic syndrome: prediction, plasticity, and programming. Physiol Rev 85:571–633
4. **Martin-Gronert MS, Ozanne SE** 2007 Experimental IUGR and later diabetes. J Intern Med 261:437–452
5. **Jaquet D, Deghmoun S, Chevenne D, Collin D, Czernichow P, Lévy-Marchal C** 2005 Dynamic change in adiposity from fetal to postnatal life is involved in the metabolic syndrome associated with reduced fetal growth. Diabetologia 48:849–855
6. **Hales CN, Barker DJ** 2001 The thrifty phenotype hypothesis. Br Med Bull 60:5–20
7. **Limesand SW, Rozance PJ, Zerbe GO, Hutton JC, Hay Jr WW** 2006 Attenuated insulin release and storage in fetal sheep pancreatic islets with intrauterine growth restriction. Endocrinology 147:1488–1497

8. **Farrag HM, Nawrath LM, Healey JE, Dorcus EJ, Rapoza RE, Oh W, Cowett RM** 1997 Persistent glucose production and greater peripheral sensitivity to insulin in the neonate *vs.* the adult. Am J Physiol 272:E86–E93
9. **Limesand SW, Rozance PJ, Smith D, Hay Jr WW** 2007 Increased insulin sensitivity and maintenance of glucose utilization rates in fetal sheep with placental insufficiency and intrauterine growth restriction. Am J Physiol Endocrinol Metab 293:E1716–E1725
10. **Vuguin P, Raab E, Liu B, Barzilai N, Simmons R** 2004 Hepatic insulin resistance precedes the development of diabetes in a model of intrauterine growth retardation. Diabetes 53:2617–2622
11. **Vuguin PM** 2007 Animal models for small for gestational age and fetal programming of adult disease. Horm Res 68:113–123
12. **Taniguchi CM, Emanuelli B, Kahn CR** 2006 Critical nodes in signalling pathways: insights into insulin action. Nat Rev Mol Cell Biol 7:85–96
13. **Shaw RJ, Cantley LC** 2006 Ras, PI(3)K and mTOR signalling controls tumour cell growth. Nature 441:424–430
14. **Wullschleger S, Loewith R, Hall MN** 2006 TOR signaling in growth and metabolism. Cell 124:471–484
15. **Hay N, Sonenberg N** 2004 Upstream and downstream of mTOR. Genes Dev 18:1926–1945
16. **Ozcan U, Ozcan L, Yilmaz E, Düvel K, Sahin M, Manning BD, Hotamisligil GS** 2008 Loss of the tuberous sclerosis complex tumor suppressors triggers the unfolded protein response to regulate insulin signaling and apoptosis. Mol Cell 29:541–551
17. **Hardie DG** 2007 AMP-activated/SNF1 protein kinases: conserved guardians of cellular energy. Nat Rev Mol Cell Biol 8:774–785
18. **Harwood FC, Shu L, Houghton PJ** 2008 mTORC1 signaling can regulate growth factor activation of p44/42 mitogen-activated protein kinases through protein phosphatase 2A. J Biol Chem 283:2575–2585
19. **Hanson RW, Reshef L** 1997 Regulation of phosphoenolpyruvate carboxykinase (GTP) gene expression. Annu Rev Biochem 66:581–611
20. **Yoon JC, Puigserver P, Chen G, Donovan J, Wu Z, Rhee J, Adelmant G, Stafford J, Kahn CR, Granner DK, Newgard CB, Spiegelman BM** 2001 Control of hepatic gluconeogenesis through the transcriptional coactivator PGC-1. Nature 413:131–138
21. **Rodgers JT, Lerin C, Haas W, Gygi SP, Spiegelman BM, Puigserver P** 2005 Nutrient control of glucose homeostasis through a complex of PGC-1α and SIRT1. Nature 434:113–118
22. **Herzig S, Long F, Jhala US, Hedrick S, Quinn R, Bauer A, Rudolph D, Schutz G, Yoon C, Puigserver P, Spiegelman B, Montminy M** 2001 CREB regulates hepatic gluconeogenesis through the coactivator PGC-1. Nature 413:179–183
23. **Feige JN, Lagouge M, Canto C, Strehle A, Houten SM, Milne JC, Lambert PD, Mataki C, Elliott PJ, Auwerx J** 2008 Specific SIRT1 activation mimics low energy levels and protects against diet-induced metabolic disorders by enhancing fat oxidation. Cell Metab 8:347–358
24. **Puigserver P, Rhee J, Donovan J, Walkey CJ, Yoon JC, Oriente F, Kitamura Y, Altomonte J, Dong H, Accili D, Spiegelman BM** 2003 Insulin-regulated hepatic gluconeogenesis through FOXO1-PGC-1α interaction. Nature 423:550–555
25. **Gerhart-Hines Z, Rodgers JT, Bare O, Lerin C, Kim SH, Mostoslavsky R, Alt FW, Wu Z, Puigserver P** 2007 Metabolic control of muscle mitochondrial function and fatty acid oxidation through SIRT1/PGC-1α. EMBO J 26:1913–1923
26. **Horike N, Sakoda H, Kushiyama A, Ono H, Fujishiro M, Kamata H, Nishiyama K, Uchijima Y, Kurihara Y, Kurihara H, Asano T** 2008 AMPK activation increases phosphorylation of GSK3β and thereby reduces CRE transcriptional activity and PEPCK-C gene expression in the liver. J Biol Chem 283:33902–33910
27. **Koo SH, Flechner L, Qi L, Zhang X, Screaton RA, Jeffries S, Hedrick S, Xu W, Boussouar F, Brindle P, Takemori H, Montminy M** 2005 The CREB coactivator TORC2 is a key regulator of fasting glucose metabolism. Nature 437: 1109–1111
28. **Herman MA, Kahn BB** 2006 Glucose transport and sensing in the maintenance of glucose homeostasis and metabolic harmony. J Clin Invest 116:1767–1775
29. **Regnault TR, de Vrijer B, Galan HL, Wilkening RB, Battaglia FC, Meschia G** 2007 Development and mechanisms of fetal hypoxia in severe fetal growth restriction. Placenta 28:714–723
30. **de Vrijer B, Regnault TR, Wilkening RB, Meschia G, Battaglia FC** 2004 Placental uptake and transport of ACP, a neutral nonmetabolizable amino acid, in an ovine model of fetal growth restriction. Am J Physiol Endocrinol Metab 287:E1114–E1124
31. **Bonds DR, Anderson S, Meschia G** 1980 Transplacental diffusion of ethanol under steady state conditions. J Dev Physiol 2:409–416
32. **Meschia G, Battaglia FC, Hay WW, Sparks JW** 1980 Utilization of substrates by the ovine placenta *in vivo*. Fed Proc 39:245–249
33. **Burd LI, Jones Jr MD, Simmons MA, Makowski EL, Meschia G, Battaglia FC** 1975 Placental production and foetal utilisation of lactate and pyruvate. Nature 254:710–711
34. **Mellor DJ, Matheson IC** 1979 Daily changes in the curved crown-rump length of individual sheep fetuses during the last 60 days of pregnancy and effects of different levels of maternal nutrition. Q J Exp Physiol Cogn Med Sci 64:119–131
35. **Regnault TR, de Vrijer B, Galan HL, Davidsen ML, Trembler KA, Battaglia FC, Wilkening RB, Anthony RV** 2003 The relationship between transplacental O2 diffusion and placental expression of PlGF, VEGF and their receptors in a placental insufficiency model of fetal growth restriction. J Physiol 550:641–656
36. **Nagatani S, Zeng Y, Keisler DH, Foster DL, Jaffe CA** 2000 Leptin regulates pulsatile luteinizing hormone and growth hormone secretion in the sheep. Endocrinology 141:3965–3975
37. **Rozance PJ, Limesand SW, Barry JS, Brown LD, Thorn SR, LoTurco D, Regnault TR, Friedman JE, Hay Jr WW** 2008 Chronic late-gestation hypoglycemia upregulates hepatic PEPCK associated with increased PGC1α mRNA and phosphorylated CREB in fetal sheep. Am J Physiol Endocrinol Metab 294: E365–E370
38. **Zhu MJ, Han B, Tong J, Ma C, Kimzey JM, Underwood KR, Xiao Y, Hess BW, Ford SP, Nathanielsz PW, Du M** 2008 AMP-activated protein kinase signalling pathways are down regulated and skeletal muscle development impaired in fetuses of obese, over-nourished sheep. J Physiol 586:2651–2664
39. **Brown LD, Rozance PJ, Barry JS, Friedman JE, Hay Jr WW** 2009 Insulin is required for amino acid stimulation of dual pathways for translational control in skeletal muscle in the late gestation ovine fetus. Am J Physiol Endocrinol Metab 296:E56–E63
40. **Cunningham JT, Rodgers JT, Arlow DH, Vazquez F, Mootha VK, Puigserver P** 2007 mTOR controls mitochondrial oxidative function through a YY1-PGC-1alpha transcriptional complex. Nature 450:736–740
41. **Simmons RA** 2007 Developmental origins of β-cell failure in type 2 diabetes: the role of epigenetic mechanisms. Pediatr Res 61:64R–67R
42. **Ross JC, Fennessey PV, Wilkening RB, Battaglia FC, Meschia G** 1996 Placental transport and fetal utilization of leucine in a model of fetal growth retardation. Am J Physiol 270:E491–E503
43. **Carver TD, Quick AA, Teng CC, Pike AW, Fennessey PV, Hay Jr WW** 1997 Leucine metabolism in chronically hypoglycemic hypoinsulinemic growth-restricted fetal sheep. Am J Physiol 272:E107–E117
44. **Raught B, Gingras AC** 1999 eIF4E activity is regulated at multiple levels. Int J Biochem Cell Biol 31:43–57
45. **Zhu MJ, Ford SP, Nathanielsz PW, Du M** 2004 Effect of maternal nutrient restriction in sheep on the development of fetal skeletal muscle. Biol Reprod 71:1968–1973
46. **Mauvais-Jarvis F, Ueki K, Fruman DA, Hirshman MF, Sakamoto K, Goodyear LJ, Iannacone M, Accili D, Cantley LC, Kahn CR** 2002 Reduced expression of the murine p85α subunit of phosphoinositide 3-kinase improves insulin signaling and ameliorates diabetes. J Clin Invest 109:141–149
47. **Cornier MA, Bessesen DH, Gurevich I, Leitner JW, Draznin B** 2006 Nutritional upregulation of p85α expression is an early molecular manifestation of insulin resistance. Diabetologia 49:748–754
48. **Bandyopadhyay GK, Yu JG, Ofrecio J, Olefsky JM** 2005 Increased p85/55/50 expression and decreased phosphotidylinositol 3-kinase activity in insulin-resistant human skeletal muscle. Diabetes 54:2351–2359
49. **Barbour LA, Mizanoor Rahman S, Gurevich I, Leitner JW, Fischer SJ, Roper MD, Knotts TA, Vo Y, McCurdy CE, Yakar S, Leroith D, Kahn CR, Cantley LC, Friedman JE, Draznin B** 2005 Increased P85α is a potent negative regulator of skeletal muscle insulin signaling and induces *in vivo* insulin resistance associated with growth hormone excess. J Biol Chem 280:37489–37494
50. **Ozanne SE, Jensen CB, Tingey KJ, Storgaard H, Madsbad S, Vaag AA** 2005 Low birthweight is associated with specific changes in muscle insulin-signalling protein expression. Diabetologia 48:547–552
51. **Calera MR, Pilch PF** 1998 Induction of Akt-2 correlates with differentiation in Sol8 muscle cells. Biochem Biophys Res Commun 251:835–841
52. **Vandromme M, Rochat A, Meier R, Carnac G, Besser D, Hemmings BA, Fernandez A, Lamb NJ** 2001 Protein kinase Bβ/Akt2 plays a specific role in muscle differentiation. J Biol Chem 276:8173–8179
53. **Sumitani S, Goya K, Testa JR, Kouhara H, Kasayama S** 2002 Akt1 and Akt2 differently regulate muscle creatine kinase and myogenin gene transcription in insulin-induced differentiation of C2C12 myoblasts. Endocrinology 143:820–828
54. **Héron-Milhavet L, Franckhauser C, Rana V, Berthenet C, Fisher D, Hemmings BA, Fernandez A, Lamb NJ** 2006 Only Akt1 is required for proliferation, while Akt2 promotes cell cycle exit through p21 binding. Mol Cell Biol 26:8267–8280
55. **Tureckova J, Wilson EM, Cappalonga JL, Rotwein P** 2001 Insulin-like growth factor-mediated muscle differentiation: collaboration between phosphatidylinositol 3-kinase-Akt-signaling pathways and myogenin. J Biol Chem 276: 39264–39270

56. **Barton ER, Morris L, Musaro A, Rosenthal N, Sweeney HL** 2002 Muscle-specific expression of insulin-like growth factor I counters muscle decline in mdx mice. J Cell Biol 157:137–148
57. **Bouzakri K, Karlsson HK, Vestergaard H, Madsbad S, Christiansen E, Zierath JR** 2006 IRS-1 serine phosphorylation and insulin resistance in skeletal muscle from pancreas transplant recipients. Diabetes 55:785–791
58. **Yang ZZ, Tschopp O, Baudry A, Dümmler B, Hynx D, Hemmings BA** 2004 Physiological functions of protein kinase B/Akt. Biochem Soc Trans 32: 350–354
59. **Gwinn DM, Shackelford DB, Egan DF, Mihaylova MM, Mery A, Vasquez DS, Turk BE, Shaw RJ** 2008 AMPK phosphorylation of raptor mediates a metabolic checkpoint. Mol Cell 30:214–226
60. **Lee IH, Cao L, Mostoslavsky R, Lombard DB, Liu J, Bruns NE, Tsokos M, Alt FW, Finkel T** 2008 A role for the NAD-dependent deacetylase Sirt1 in the regulation of autophagy. Proc Natl Acad Sci USA 105:3374–3379
61. **Ron D, Walter P** 2007 Signal integration in the endoplasmic reticulum unfolded protein response. Nat Rev Mol Cell Biol 8:519–529
62. **Tsiotra PC, Tsigos C** 2006 Stress, the endoplasmic reticulum, and insulin resistance. Ann NY Acad Sci 1083:63–76
63. **Long YC, Zierath JR** 2006 AMP-activated protein kinase signaling in metabolic regulation. J Clin Invest 116:1776–1783
64. **Hay Jr WW** 2006 Recent observations on the regulation of fetal metabolism by glucose. J Physiol 572:17–24
65. **Battaglia FC, Meschia G** 1978 Principal substrates of fetal metabolism. Physiol Rev 58:499–527
66. **Das UG, Sadiq HF, Soares MJ, Hay Jr WW, Devaskar SU** 1998 Time-dependent physiological regulation of rodent and ovine placental glucose transporter (GLUT-1) protein. Am J Physiol 274:R339–R347
67. **Thureen PJ, Trembler KA, Meschia G, Makowski EL, Wilkening RB** 1992 Placental glucose transport in heat-induced fetal growth retardation. Am J Physiol 263:R578–R585
68. **Wallace JM, Milne JS, Aitken RP, Hay Jr WW** 2007 Sensitivity to metabolic signals in late-gestation growth-restricted fetuses from rapidly growing adolescent sheep. Am J Physiol Endocrinol Metab 293:E1233–E1241
69. **Owens JA, Gatford KL, De Blasio MJ, Edwards LJ, McMillen IC, Fowden AL** 2007 Restriction of placental growth in sheep impairs insulin secretion but not sensitivity before birth. J Physiol 584:935–949
70. **Ford SP, Hess BW, Schwope MM, Nijland MJ, Gilbert JS, Vonnahme KA, Means WJ, Han H, Nathanielsz PW** 2007 Maternal undernutrition during early to mid-gestation in the ewe results in altered growth, adiposity, and glucose tolerance in male offspring. J Anim Sci 85:1285–1294
71. **De Blasio MJ, Gatford KL, Robinson JS, Owens JA** 2007 Placental restriction of fetal growth reduces size at birth and alters postnatal growth, feeding activity, and adiposity in the young lamb. Am J Physiol 292:R875–R886
72. **De Blasio MJ, Gatford KL, McMillen IC, Robinson JS, Owens JA** 2007 Placental restriction of fetal growth increases insulin action, growth, and adiposity in the young lamb. Endocrinology 148:1350–1358
73. **Gardner DS, Tingey K, Van Bon BW, Ozanne SE, Wilson V, Dandrea J, Keisler DH, Stephenson T, Symonds ME** 2005 Programming of glucose-insulin metabolism in adult sheep after maternal undernutrition. Am J Physiol 289: R947–R954
74. **Lane RH, Flozak AS, Ogata ES, Bell GI, Simmons RA** 1996 Altered hepatic gene expression of enzymes involved in energy metabolism in the growth-retarded fetal rat. Pediatr Res 39:390–394
75. **Desai M, Byrne CD, Zhang J, Petry CJ, Lucas A, Hales CN** 1997 Programming of hepatic insulin-sensitive enzymes in offspring of rat dams fed a protein-restricted diet. Am J Physiol 272:G1083–G1090